Journal of Radiation Research, Vol. 57, No. 6, 2016, pp. 637–645
doi: 10.1093/jrr/rrw072
Advance Access Publication: 7 September 2016

Dosimetric impact of an air passage on intraluminal brachytherapy for bronchus cancer

Hiroyuki Okamoto*, Akihisa Wakita, Satoshi Nakamura, Shie Nishioka, Ako Aikawa, Toru Kato, Yoshihisa Abe, Kazuma Kobayashi, Koji Inaba, Naoya Murakami and Jun Itami

Department of Radiation Oncology, National Cancer Center Hospital, 5-1-1 Tsukiji, Chuo-ku, Tokyo 104-0045, Japan
*Corresponding author. Department of Radiation Oncology, National Cancer Center Hospital, 5-1-1 Tsukiji, Chuo-ku, Tokyo 104-0045, Japan.
Tel: +81-3-3542-2511; Fax: +81-3-3545-3567; Email: hiokamot@ncc.go.jp
Received October 22, 2015; Revised February 16, 2016; Accepted May 17, 2016

ABSTRACT

The brachytherapy dose calculations used in treatment planning systems (TPSs) have conventionally been performed assuming homogeneous water. Using measurements and a Monte Carlo simulation, we evaluated the dosimetric impact of an air passage on brachytherapy for bronchus cancer. To obtain the geometrical characteristics of an air passage, we analyzed the anatomical information from CT images of patients who underwent intraluminal brachytherapy using a high-dose-rate ^{192}Ir source (MicroSelectron V2r®, Nucletron). Using an ionization chamber, we developed a measurement system capable of measuring the peripheral dose with or without an air cavity surrounding the catheter. Air cavities of five different radii (0.3, 0.5, 0.75, 1.25 and 1.5 cm) were modeled by cylindrical tubes surrounding the catheter. A Monte Carlo code (GEANT4) was also used to evaluate the dosimetric impact of the air cavity. Compared with dose calculations in homogeneous water, the measurements and GEANT4 indicated a maximum overdose of 5–8% near the surface of the air cavity (with the maximum radius of 1.5 cm). Conversely, they indicated a minimum overdose of ~1% in the region 3–5 cm from the cavity surface for the smallest radius of 0.3 cm. The dosimetric impact depended on the size and the distance of the air passage, as well as the length of the treatment region. Based on dose calculations in water, the TPS for intraluminal brachytherapy for bronchus cancer had an unexpected overdose of 3–5% for a mean radius of 0.75 cm. This study indicates the need for improvement in dose calculation accuracy with respect to intraluminal brachytherapy for bronchus cancer.

KEYWORDS: brachytherapy, heterogeneity, TPS, HDR, TG-43

INTRODUCTION

High-dose-rate (HDR) brachytherapy plays an important role in current radiotherapy, specifically for cervical, prostate and breast cancer treatments [1]. For the dosimetric characteristic of HDR brachytherapy, a radioactive source such as ^{192}Iridium (^{192}Ir) provides a very high dose to the tumors while sparing unwanted dose to the healthy organs surrounding it, because the dose gradient around a brachytherapy source is very steep and the dose decreases exponentially with the thickness of the material or tissue. Moreover, brachytherapy can achieve high accuracy through the well-established remote afterloading system, capable of accurately transferring the radioactive source [2].

Since its inception, the brachytherapy dose calculations used in treatment planning systems (TPSs) have conventionally been based on the dose distribution from a single source in homogeneous water according to the AAPM Task Group 43 (TG-43U1) [3–6]. Hence, clinical experiences have been accumulated for dosimetric parameters calculated by the TG-43U1 protocol. Recently, many researchers have investigated the dosimetric impact in a heterogeneous medium or the applicators through either measurements or Monte Carlo studies. A discrepancy between the TPS dose and the actual dose can potentially appear under various conditions, and this should be clarified accurately to correlate the clinical outcome to dosimetric parameters.

As shown in Fig. 1, in brachytherapy for bronchus cancer, there exists a heterogeneous structure, an air passage surrounding the treatment region. Our purpose here was to evaluate the dosimetric

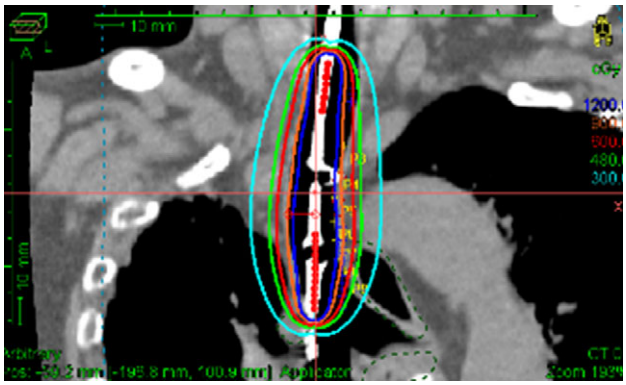

Fig. 1. An example of a treatment plan for bronchus cancer using a Lumencath catheter.

impact due to the presence of the air passage through both measurements and Monte Carlo simulations. We have developed a measurement system capable of measuring the peripheral dose surrounding the catheter, with or without the presence of an air cavity, using a miniaturized ionization chamber. In addition, for assessment of the dosimetric impact under those condition, a ^{192}Ir was modeled in a GEANT4 Monte Carlo code [7], which is widely used for research in radiotherapy, including brachytherapy [8–12].

MATERIALS AND METHODS

Air passage for bronchus cancer

To obtain the geometrical characteristics of an air passage, delineation of the air passage had been conducted on CT-images of patients. These patients underwent intraluminal brachytherapy for early-stage bronchus cancer using a high-dose-rate ^{192}Ir source (MicroSelectron V2r®, Nucletron, an Elekta company, Stockholm, Sweden) at our institution. This investigation was approved by our Institutional Review Board. The air passage surrounding a Lumencath catheter was recreated as a contoured structure defined as threshold segmentation from a CT value of −1000 to −150 HU in the TPS Oncentra®Brachy (Ver. 4.1.0.132, Nucletron). Afterward, we manually deleted parts of the structure protruding from the treatment region, which was defined as the source active length L_{act}. Next, we measured the maximum radius R_{max} by visual evaluation and obtained the volume of the air passage V. A mean radius R_{mean} could be derived from V and L_{act}. Table 1 shows the geometrical characteristics of the air passage for bronchus cancer patients ($n = 6$).

Measurement system

As shown in Fig. 2a, we developed a measurement system that consisted of a single catheter (5Fr flexible needle, Nucletron) inserted in a cylindrical tube and a miniaturized ionization chamber (31 010 Semiflex chamber, PTW, Freiburg Germany) in a water phantom. The cylindrical tube, which normally contains water, can be used to simulate an air passage by removing the water. As shown in Fig. 2b, cylindrical tubes with a wall thickness of 3 mm were made with five inner radii, R_{air} = 0.3, 0.5, 0.75, 1.25 and 1.5 cm, taking into consideration the geometrical characteristics of air passages (see Table 1). The pit in the bottom of the cylindrical tube was used for the fixation of the plastic needle (Fig. 2c). The tube was made of a water-equivalent phantom material (tough water [13], Kyoto Kagaku Co., Ltd, Kyoto, Japan).

Table 1. Geometrical characteristics of air passages for early-stage bronchus cancer patients ($n = 6$)

Patient	V (cm^3)	L_{act} (cm)	R_{max} (cm)	R_{mean} (cm)
1	6.86	4.5	0.93	0.70
2	11.17	6.0	0.91	0.77
3	25.07	9.0	1.34	0.94
4	12.44	6.5	1.46	0.78
5	3.60	3.5	1.04	0.57
6	15.60	8.5	1.60	0.76
Mean	12.46	6.3	1.21	0.75
1σ	7.49	2.2	0.29	0.12

V = volume of air passage, L_{act} = length of source activation, R_{max} = maximum radius of air passage, R_{mean} = mean radius of air passage, 1σ = a standard deviation.

The absorbed dose $D_{w,Q}$ in water was derived from

$$D_{w,Q} = M_Q N_{D,w,Q_0} k_{Q,Q_0} \quad (1)$$

where M_Q is the collected charge with corrections for the pressure and temperature k_{TP}, ion recombination k_s, and polarity effect k_{pol}, and $N_{D,w,Q_0}$is the calibration factor in terms of absorbed dose in water according to IAEA TRS-398 [14]. The beam quality symbols Q and Q_0 correspond to the ^{192}Ir and ^{60}Co gamma ray fields, respectively. The correction factor k_{TP} was applied to calculate the cavity air mass from the standard reference conditions (temperature T_0 = 22°C and pressure P_0 = 101.3 kPa). The ion recombination k_s was derived using the two-voltage method for ion recombination, as shown in Eq. (2).

$$k_s = \frac{(V_1/V_2)^2 - 1}{(V_1/V_2)^2 - (M_1/M_2)} \quad (2)$$

Here, M_1 and M_2 are the measured values of the collected charge at the voltages V_1 and V_2, respectively (V_1/V_2 = 2, V_1 = 400 V). By using Eq. (2), the ion recombination k_s at 1.0, 3.0 and 5.4 cm distance in a direction transversal to the ^{192}Ir source in water was estimated to be 1.002, 1.003 and 1.001, respectively, indicating a very small distance dependency. The mean value of 1.002 was applied to all of the measurements. The polarity effect k_{pol} at a distance of 1.0, 3.0 and 5.4 cm in a direction transversal to the ^{192}Ir source in water was 1.012, 1.005 and 1.000, respectively. In the same way, the mean value of 1.005 was applied to all of the measurements. The beam quality correction factor k_{Q,Q_0}in a direction transversal to the ^{192}Ir source for a PTW Semiflex chamber, reported by Araki [15], was applied to all of the measurements in this study.

After changing the ^{192}Ir source every 3 months, the air-kerma strength S_k was measured with a HDR-1000Plus well-type ionization chamber and MAX-4000 electrometer (Standard Imaging, Inc.

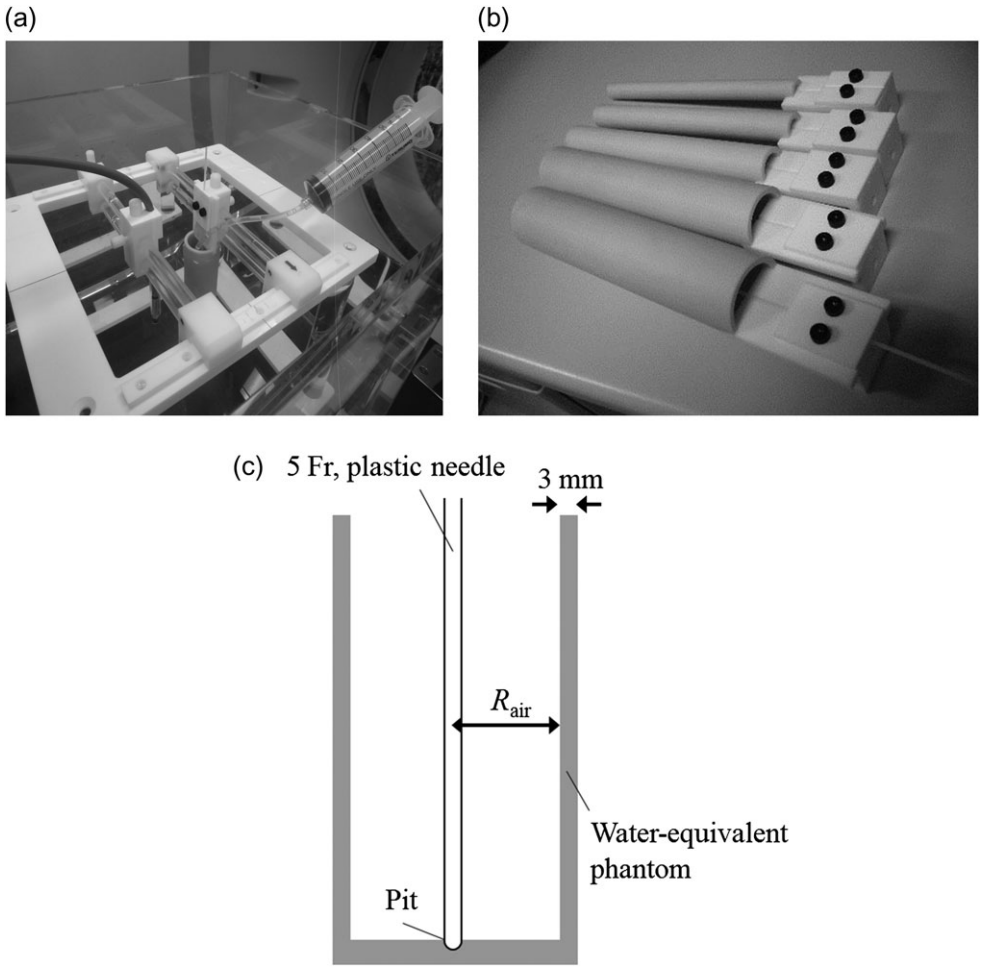

Fig. 2. (a) Flexible needle catheter inserted in the cylindrical tube and a PTW Semiflex chamber positioned in a water phantom. (b) Cylindrical tubes for five inner radii: R_{air} = 0.3, 0.5, 0.75, 1.25 and 1.5 cm. (c) Schematic view of the cylindrical tube.

WI, USA) by our staff. The calibration factor of the detector was determined by the cross-calibration using a reference detector, which was calibrated at an accredited dosimetry calibration laboratory (ADCL). The measured S_k was registered in the treatment planning systems and the console of the treatment machine.

The chamber can be freely moved by sliding a jig. However, in this study, the measurements of the peripheral dose were conducted only along a direction transversal to the ^{192}Ir source. We measured the peripheral dose under two conditions. (i) Peripheral dose in homogenous water for a single dwell position. The measured distance from the catheter was approximately 1 to 9 cm. The measured doses were compared with the calculated doses in the TPS according to the AAPM TG-43U1 protocol. (ii) Peripheral dose in the presence of an air cavity. The dosimetric impact of the air cavity was evaluated by the ratio of the peripheral dose with an air cavity to the peripheral dose without it. Multiple dwell times were determined by using geometrical optimization in the TPS. The method of treatment planning is described in the next section. The chamber was placed at the center of the source active length. The measured distance from the catheter was approximately 1–5 cm in this measurement. The dose change, caused by positioning errors of the chamber and the catheter, was reduced effectively by measuring the peripheral dose with and without an air cavity at a fixed position with respect to the chamber and the catheter. As shown in Fig. 2a, the water in the cylindrical tube was removed by a syringe without changing the relative positions. After both measurements were taken, the distance from the chamber to the catheter was changed for the next measurement.

Treatment planning

CT images of our measurement system were obtained to prepare a treatment plan. In the planning, the reference points along a catheter direction were placed 0.5 cm distant from the surface of the air cavity in the cylindrical tube (see Fig. 3a). The treatment region was 6 cm with a source step size of 0.5 cm, because the mean value of L_{act} was found to be 6.3 cm (Table 1). The center in the source active region was aligned with the position of the chamber. The dwell times were determined by geometrical optimization [16] with a prescribed dose of 200 cGy to the reference points for smoothing doses at reference points (see Fig. 3b). The treatment parameters

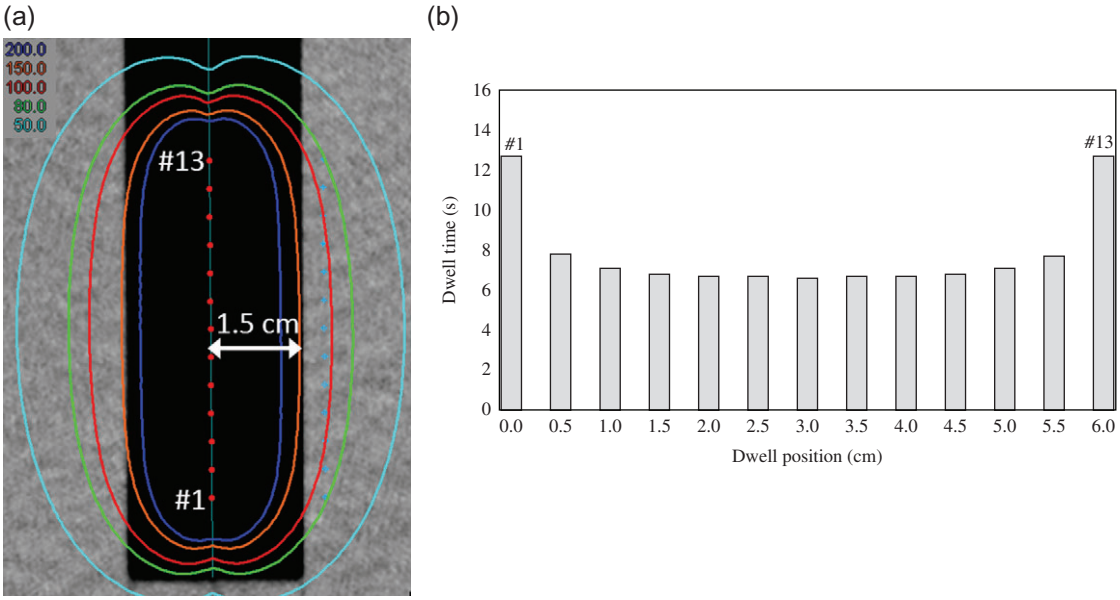

Fig. 3. (a) Treatment plan for a cylindrical tube (1.5 cm radius) with isodose curves of the percentage of the prescribed dose. (b) Distribution of the dwell times determined by geometrical optimization.

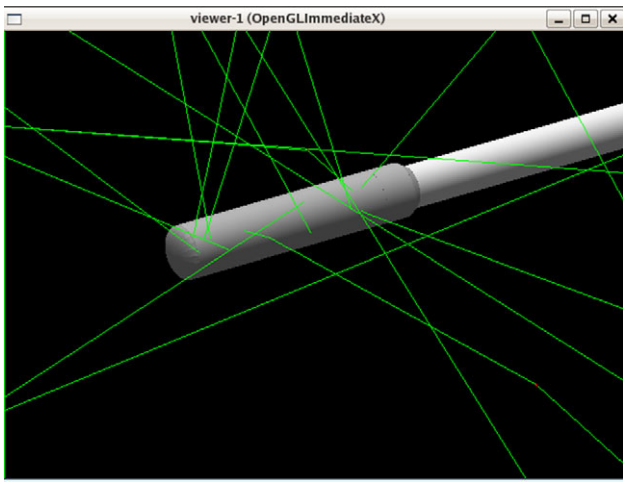

Fig. 4. Graphics of the ^{192}Ir source modeled by the GEANT4 simulation. Green lines depict the gamma rays emitted from the ^{192}Ir source.

were transferred to the console of the remote afterloading system (MicroSelectron®, Nucletron) for irradiations.

Monte Carlo simulation by GEANT4

As shown in Fig. 4, a Nucletron ^{192}Ir source was modeled in the GEANT4 Monte Carlo code (Ver. 4.8.2 p02) by using the geometrical information reported by Daskalov [17]. We used photon energy spectra for ^{192}Ir, reported by Rivard [18]. In this study, 'standard ElectroMagnetic (EM) physics' was selected for calculating the dose distribution with a range cut value of 0.4 mm. The standard EM physics was provided by the electromagnetic standard physics working group established in the GEANT4 project. The ratio of the peripheral dose with the air cavity to the peripheral dose without it was calculated for five inner radii: R_{air} = 0.3, 0.5, 0.75, 1.25 and 1.5 cm. The source active length was 6 cm and the dwell times were determined by the geometrical optimization.

The size of the water phantom was 30 × 30 × 30 cm^3 for the full scatter conditions. The sensitive detectors made of water, each with a volume of 1 × 1 × 1 mm^3, can store the energy deposited by the interactions. The dose distribution along the transversal direction of the source at the center of the source active length was obtained from the accumulation of the energy deposited in the sensitive detectors. The GEANT4 simulation was performed by non-parallel computation on an Intel (R) Core (TM) i7-3930K CPU in a workstation (INVERSENET INC. Tokyo, Japan). It took several days to obtain a single dose distribution.

RESULTS

Measurements of absorbed dose in homogeneous water

As shown in Fig. 5, the absorbed dose for a single dwell position in homogenous water was measured with the PTW Semiflex chamber along a transversal direction of the ^{192}Ir source (generally written $\theta = \pi/2$ in TG-43U1). The local dose differences between the measured dose and the TPS dose based on TG-43U1 at a distance of 1.0, 2.0, 3.0, 5.4, 6.8 and 9.1 cm from the ^{192}Ir source were 9.0%, 4.8%, 4.6%, 0.2%, 1.3% and 2.0%, respectively.

Measurement of dosimetric impact due to an air cavity

Figure 6 shows the local dose difference between the measured dose with and without an air cavity for multiple dwell positions. The location of the dose distributions corresponds to the center of the source active length of 6 cm. The dwell times were determined by geometrical optimization in the TPS. The horizontal axis corresponds to the distance from the surface of the air cavity in the cylindrical tube. Local dose

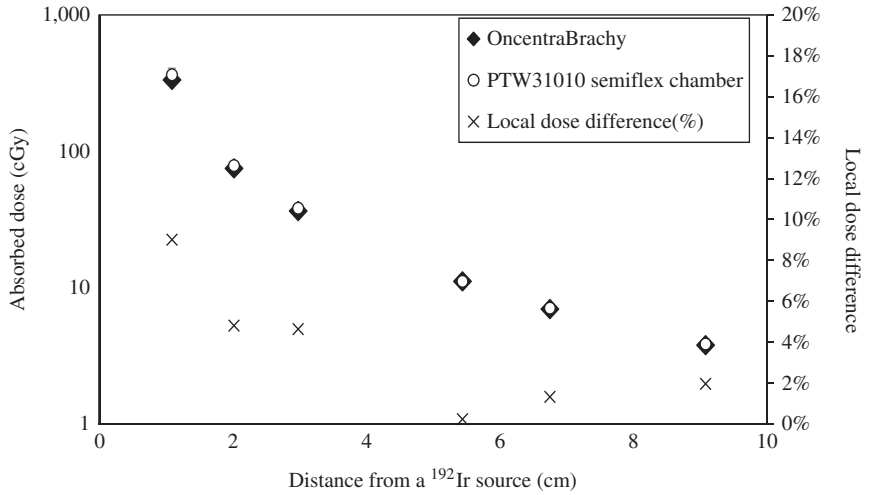

Fig. 5. Absorbed dose for a single dwell position in homogenous water, measured with a PTW Semiflex chamber at a dwell time of 35 s with an air-kerma strength of 29.97 mGy m^2 h^{-1}. The local dose difference is also shown on the right vertical axis. The expanded measurement uncertainty (coverage factor $k = 1$) at a distance of 1.0, 3.0 and 5.0 cm from the ^{192}Ir source was 12%, 4% and 3%, respectively.

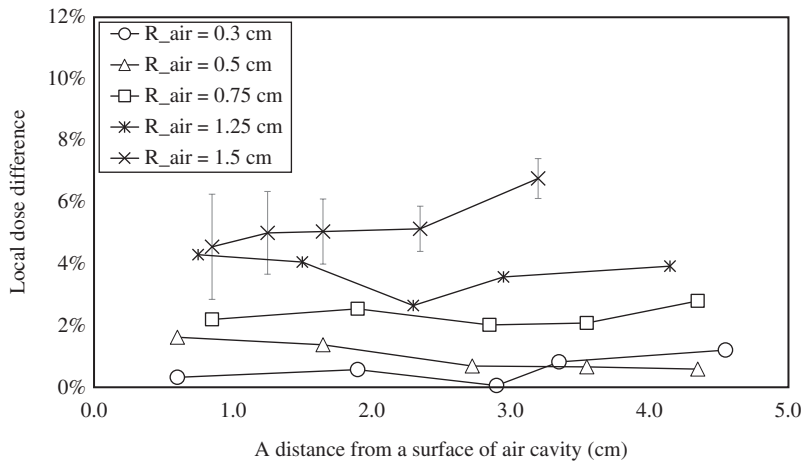

Fig. 6. Local dose difference along a transversal direction of the ^{192}Ir source between the dose with and without an air cavity for five inner radii, R_{air}. The expanded measurement uncertainty (coverage factor $k = 1$) at a distance of 1.0, 3.0 and 5.0 cm from the ^{192}Ir source was 4%, 1% and <1%, respectively.

differences increase with increasing radius of the air cavity. The maximum local dose difference was found to be 6.8% at a distance of 3.2 cm for the maximal 1.5 cm radius. Furthermore, little dependency on the distance from the surface of the air cavity was observed, except for R_{air} = 1.5 cm. The mean local dose differences in the entire region for R_{air} = 0.3, 0.5, 0.75, 1.25 and 1.5 cm were 0.6%, 1.0%, 2.3%, 3.7% and 5.3%, respectively.

Monte Carlo simulation by GEANT4

Figure 7 shows the dose distribution in the Oncentra®Brachy and the dose distribution with and without the cylindrical air cavity (R_{air} = 1.5 cm) for multiple dwell positions, calculated by the GEANT4 simulation. The location of the dose distributions corresponds to the center of the source active length of 6 cm. The local dose differences in water between the GEANT4 and the TPS are also shown on the right vertical axes (open squares), and the mean and standard deviation was 0.5 ± 0.3%. The figure also shows dose changes due to the air cavity (closed squares), and it indicates large increases over ~5%, which is similar to the results of the measurements. Furthermore, we derived the mean local dose differences for each size of the cylindrical air cavity in four different regions, at 0–0.5, 0.5–1, 1.5–3 and 3–5 cm distances from the surface of the cylindrical cavity (see Fig. 8). Compared with dose calculations in homogeneous water, large overdoses were observed, particularly for a large air cavity radius. The GEANT4 simulation shows a maximum 7.5% overdose in the nearest region (0–0.5 cm) for the

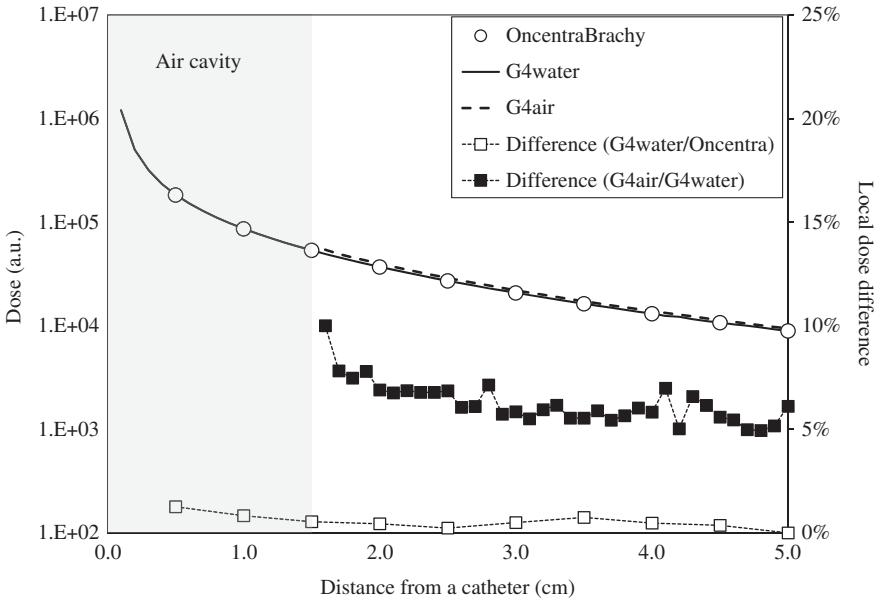

Fig. 7. Dose distribution in the Oncenrea®Brachy (open circles). Dose at a 5 cm distance was normalized to the dose in water by GEANT4. Dose distributions with (dashed line) and without (solid line) the cylindrical air cavity for a maximum radius of 1.5 cm, calculated by the GEANT4 simulation. The open and closed squares are local dose differences, which are shown on the right vertical axes.

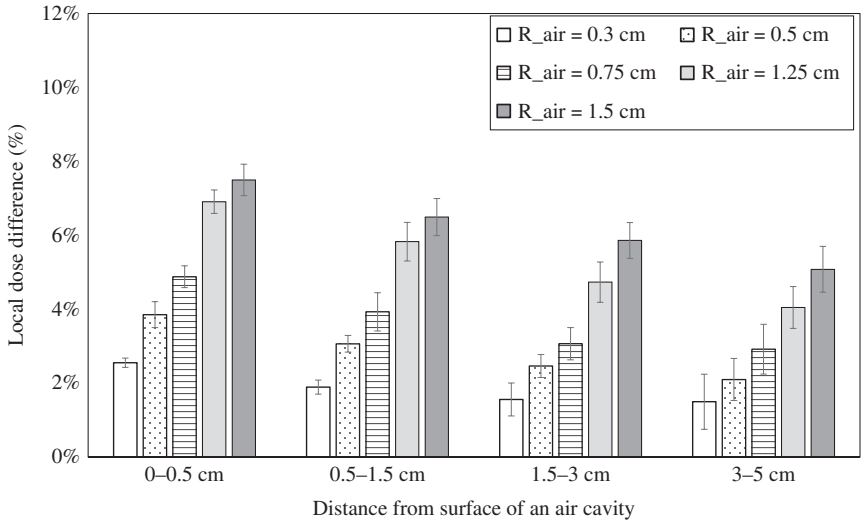

Fig. 8. Local dose differences between dose distributions with and without an air cavity in four different regions, calculated by the GEANT4 simulation.

largest radius, i.e. 1.5 cm. Conversely, it shows a minimum 1.5% overdose in the farthest region (3–5 cm) for the smallest radius of 0.3 cm. Furthermore, the overdoses depend on the distance from the air cavity.

DISCUSSION

According to the GUM report [19], measurement uncertainties in this study were estimated for two experiments: (i) measurements of the absorbed dose in homogeneous water and (ii) dose change with or without the air cavity in the cylindrical tube. (i) The uncertainty in the calibration factor N_{D,w,Q_0} and beam quality k_{Q,Q_0} was 1.5% and 1.1%, respectively [15]. In brachytherapy, there is a large uncertainty in the positional accuracy of the source and the detector. If a positioning displacement potentially occurs within ±1 mm, the dose change at a distance of 1.0, 3.0 and 5.0 cm from the catheter would vary by approximately ±20%, ±7% and ±4%, respectively, by the

inverse square law. For the derivation of the uncertainty, the probability was assumed to be a rectangular distribution. The combined uncertainty for the other correction factors, k_{pol}, k_s and k_{TP} was ~0.6%. From these results, the expanded measurement uncertainty (coverage factor $k = 1$) for the distances was estimated to be 12%, 4% and 3%, respectively in this measurement. This is because Fig. 5 shows a large difference near the source, but these differences are within the uncertainties. In addition, the trend of the result was similar to one study reported by Araki *et al.* [15], and large dose differences were observed in a close range from the source. A dedicated device such as the sandwich method is necessary for further improvement of the positional accuracy near the source. Gromoll *et al.* [20] measured the radial dose function and the anisotropic function in the close range (0.5 cm) using a PTW pinpoint chamber. There was a large deviation of ~10% among several measurements for the anisotropic function. In a similar study, Patel *et al.* [21] measured the radial dose function using a PTW Semiflex chamber for a different normalizing point, with a distance of 1 and 5 cm from the source, and the standard deviations were found to be 2–5% and 2%, respectively. A larger deviation was observed at the 1 cm normalizing point. Dose change due to the positional inaccuracy decreases with increasing distance from the source. Sarfehnia *et al.* [22] measured the absorbed dose at a 5 cm distance from the source in water with an ionization chamber, and a −1.4% dose difference was observed (reference: TG-43). In this study, the mean dose difference was 1.2% in the distance range of 5 to 9 cm. (ii) This measurement is expected to be less influenced by positional inaccuracy, because the relative position was not changed for the measurements with and without the air cavity. Therefore, the source position accuracy was estimated by the geometrical error from the 1.5 mm inner diameter of the needle and the 0.9 mm diameter of the ^{192}Ir source. As a result, the expanded measurement uncertainty at a distance of 1.0, 3.0 and 5.0 cm was estimated to be 4%, 1% and <1%. In addition, the TPS dose based on TG-43U1 had calculation uncertainties: a measurement uncertainty of 1.5% in air-kerma strength S_k and a TPS interpolation uncertainty of 2.6%. Thus, the total dose calculation uncertainty could be estimated to be 3.4% in the dose at 1 cm in the transverse plane [23]. The GEANT4 simulation shows a calculation uncertainty of within 1%, estimated from the standard deviation of energy deposited in each sensitive detector for a single dose distribution. The error bar is shown in Fig. 8. Figure 7 shows that the local dose differences in water between the Oncentra®Brachy and the GEANT4 were within the calculation uncertainty of 1% in the GEANT4. Hence, dose calculation accuracy in water by GEANT4 is comparable with that of the TPS.

The dosimetric impact of the air passage depends on the size and the distance of the air passage, as well as the length of treatment region corresponding to the source active length. For instance, as shown in Fig. 8, local dose differences increased slightly closer to the air cavity. The radiation path length through the air cavity can be identified as a cause for this distance dependence of the overdoses. In the region close to the air cavity, the path length through the air cavity can become greater for dwell positions far from the center of the source active length. This can result in a greater overdose in the region closer to the air cavity. Therefore, the GEANT4 simulation shows a 4.9% overdose in the 0–0.5 cm region and a 2.9% overdose in the 3–5 cm region for R_{air} = 0.75 cm. This distance dependence of overdoses could not be fully observed in the measurements because of the accuracy limit in the positioning of the chamber and the catheter.

The dedicated catheter for bronchus cancer in intraluminal brachytherapy has wings around the treatment region, which enables a centered position of the catheter in the lumen to avoid occurrence of an unwanted high dose in the wall of the trachea and bronchus. The radius of the wing is approximately 0.6–0.75 cm, and this could correspond to the mean radii of an air passage, as shown in Table 1. The mean and maximum radii of the air passage for bronchus cancer were found to be 0.75 and 1.6 cm, corresponding to 3–5% and 5–8% overdose within a 5 cm distance from the air passage, respectively, by reference to calculations from a GEANT4 simulation (Fig. 8).

Recently, our group investigated the late complication events for patients who underwent endobronchial brachytherapy in our institution [24, 25], and we further extracted a dosimetric parameter, such as $D_{2\,cm^3}$ in equivalent dose to 2 Gy (EQD_2), to reveal a relation between the dosimetric parameters and the late complications rate, as reported by Murakami *et al.* [24]. As a result, it was discovered that $D_{2\,cm^3} > 85$ Gy in EQD_2 for the trachea and the main bronchus is a strong risk factor in relation to severe late respiratory complication. The clinical effect due to such overdoses being received is still unknown and is being investigated in clinical practice.

Model-based dose calculation methods, such as the collapsed-cone convolution [26] and grid-based Boltzmann solver [27, 28], which have better dose calculation accuracies in a heterogeneous medium or applicators, have been developed and researched [29, 30]. There is much research [31–34] investigating dosimetric discrepancies in specific situations, such as a metallic applicator or needle, rectal heterogeneity, skin dose in a finite patient dimension, and an air cavity of SAVI^{TM}. For instance, the SAVI^{TM} applicator is used to deliver partial breast irradiation and is placed inside the lumpectomy cavity. The dosimetric impact of the air cavity affects the area around the treatment region, as discussed in this study. From Ref. [33], the peripheral dose indicated 3–9% overdoses due to the presence of the air cavity; the overdose can increase with increasing size of the air cavity. The dose difference at a 1 cm distance from the catheter for 1.5, 2.0 and 2.5 cm radii of the SAVI^{TM} was 3.6%, 6% and 8.3%, respectively (Table II in Ref. [33]). The trend of their results is similar to that of our results, but the dose differences are lower than ours. This is because the air cavity in SAVI^{TM} is spherical, not cylindrical, as in ours.

The clinical brachytherapy uncertainty is estimated to be 8–13%, as reported by Kirisits [35]. Therefore, the 3–5% overdoses caused in intraluminal brachytherapy should be considered; these results indicate the need for improvement in dose calculation accuracy in intraluminal brachytherapy for bronchus cancer.

CONCLUSION

The dosimetric impact of the presence of an air passage depended on the size of the air passage, the treatment length, and the distance from the air passage. In clinical practice, the mean radius of the air

passage is found to be ~0.75 cm for bronchus cancer. In that case, the TPS based on dose calculation in homogeneous water had an unexpected overdose of 3–5% in intraluminal brachytherapy for bronchus cancer. This study indicated the need for improvement in dose calculation accuracy in intraluminal brachytherapy.

FUNDING

This research is partially supported by the Japan Agency for Medical Research and development, AMED (Grant Number 16ck0106039h0002) and Grant-in-Aid for Young Scientists (B) from Ministry of Education, Culture, Sports, Science and Technology (Grant Number 26860411).

ACKNOWLEDGEMENTS

The authors would like to thank all of the staff involved in brachytherapy at our institution.

CONFLICT OF INTEREST

There is no ethical problem or conflict of interest with regard to this manuscript.

REFERENCES

1. Thomadsen BR, Williamson JF, Rivard MJ, et al. Anniversary paper: past and current issues, and trends in brachytherapy physics. *Med Phys* 2008;35:4708–23.
2. Okamoto H, Aikawa A, Wakita A, et al. Dose error from deviation of dwell time and source position for high dose-rate ^{192}Ir in remote afterloading system. *J Radiat Res* 2014;55:780–7.
3. Nath R, Anderson LL, Luxton G, et al. Dosimetry of interstitial brachytherapy sources: recommendations of the AAPM Radiation Therapy Committee Task Group No. 43. American Association of Physicists in Medicine. *Med Phys* 1995;22: 209–34.
4. Rivard MJ, Coursey BM, DeWerd LA, et al. Update of AAPM Task Group No. 43 Report: a revised AAPM protocol for brachytherapy dose calculations. *Med Phys* 2004;31:633–74.
5. Rivard MJ, Butler WM, DeWerd LA, et al. Supplement to the 2004 update of the AAPM Task Group No. 43 Report. *Med Phys* 2007;34:2187–205.
6. Perez-Calatayud J, Ballester F, Das RK, et al. Dose calculation for photon-emitting brachytherapy sources with average energy higher than 50 keV: report of the AAPM and ESTRO. *Med Phys* 2012;39:2904–29.
7. Agostinelli S, Allison J, Amako K, et al. GEANT4—a simulation toolkit. *Nucl Instrum Methods Phys Res A* 2003;506:250–303.
8. Okamoto H, Kanai T, Kase Y, et al. Relation between lineal energy distribution and relative biological effectiveness for photon beams according to the microdosimetric kinetic model. *J Radiat Res* 2011;52:75–81.
9. Okamoto H, Kohno T, Kanai T, et al. Microdosimetric study on influence of low energy photons on relative biological effectiveness under therapeutic conditions using 6 MV linac. *Med Phys* 2011;38:4714–22.
10. Okamoto H, Fujita Y, Sakama K, et al. Commissioning of 6 MV medical linac for dynamic MLC-based IMRT on Monte Carlo code GEANT4. *Radiol Phys Technol* 2014;7:246–53.
11. Afsharpour H, Landry G, D'Amours M, et al. ALGEBRA: ALgorithm for the heterogeneous dosimetry based on GEANT4 for BRAchytherapy. *Phys Med Biol* 2012;57:3273–80.
12. Jiang H, Paganetti H. Adaptation of GEANT4 to Monte Carlo dose calculations based on CT data. *Med Phys* 2004;31:2811–8.
13. Araki F. Absorbed dose to water reference dosimetry using various water-equivalent solid phantoms in high-energy photon and electron beams. *Nihon Hoshasen Gijutsu Gakkai Zasshi* 2010;66 (12):1678.
14. IAEA. Absorbed dose determination in external beam radiotherapy: an international code of practice for dosimetry based on standards of absorbed dose to water. *Technical Reports Series No. 398*. International Atomic Energy Agency, Vienna, 2000.
15. Araki F, Kouno T, Ohno T et al. Measurement of absorbed dose-to-water for an HDR ^{192}Ir source with ionization chambers in a sandwich setup. *Med Phys* 2013;40:92101–8.
16. Mould RF, Battermann JJ, Martinez AA, et al. (eds). *Brachytherapy From Radium to Optimization*. Veenendaal, The Netherlands: Nucletron International, 1994.
17. Daskalov GM, Loffler E, Williamsona JF. Monte Carlo–aided dosimetry of a new high dose-rate brachytherapy source. *Med Phys* 1998;25:2200–8.
18. Rivard MJ, Granero D, Perez-Calatayud J, et al. Influence of photon energy spectra from brachytherapy sources on Monte Carlo simulations of kerma and dose rates in water and air. *Med Phys* 2010;37:869–76.
19. JCGM 100:2008 (the Joint Committee for Guides in Metrology). *Evaluation of measurement data-Guide to the expression of uncertainty in measurement*. http://www.bipm.org/utils/common/documents/jcgm/JCGM_100_2008_E.pdf (15 May 2016, date last accessed).
20. Gromoll C, Karg A. Determination of the dose characteristics in the near area of a new type of ^{192}Ir-HDR afterloading source with a PinPoint ionization chamber. *Phys Med Biol* 2002;47: 875–87.
21. Patel NP, Majumdar B, Vijayan V. Comparative dosimetry of GammaMed Plus high-dose rate ^{192}Ir brachytherapy source. *J Med Phys* 2010;35:137–43.
22. Sarfehnia A, Kawrakow I, Seuntjens J. Direct measurement of absorbed dose to water in HDR ^{192}Ir brachytherapy: water calorimetry, ionization chamber, Gafchromic film, and TG-43. *Med Phys* 2010;37:1924–32.
23. DeWerd LA, Ibbott GS, Meigooni AS, et al. A dosimetric uncertainty analysis for photon-emitting brachytherapy sources: report of AAPM Task Group No. 138 and GEC-ESTRO. *Med Phys* 2011;38:782–801.
24. Murakami N, Kobayashi K, Nakamura S, et al. A total EQD2 greater than 85 Gy for trachea and main bronchus D2cc being associated with severe late complications after definitive endobronchial brachytherapy. *J Contemp Brachytherapy* 2015;7:363–8.
25. Kobayashi K, Murakami N, Inaba K, et al. Dose reconstruction technique using non-rigid registration to evaluate spatial correspondence between high-dose region and late radiation toxicity: a case of tracheobronchial stenosis after external beam radiotherapy combined with endotracheal brachytherapy for tracheal cancer. *J Contemp Brachytherapy* 2016;8:156–63.

26. Ahnesjö A. Collapsed cone convolution of radiant energy for photon dose calculation in heterogenous media. *Med Phys* 1989;16:577–92.
27. Gifford KA, Horton JL, Wareing TA, et al. Comparison of a finite-element multigroup discrete-ordinates code with Monte Carlo for radiotherapy calculations. *Phys Med Biol* 2006;51: 2253–65.
28. Vassiliev ON, Wareing TA, McGhee J, et al. Validation of a new grid-based Boltzmann equation solver for dose calculation in radiotherapy with photon beams. *Phys Med Biol* 2010;55: 581–98.
29. Rivard MJ, Vensalaar JLM, Beaulieu L. The evolution of brachytherapy treatment planning. *Med Phys* 2009;36:2136–53.
30. Beaulieu L, Carlsson Tedgren A, Carrier JF, et al. Report of the Task Group 186 on model-based dose calculation methods in brachytherapy beyond the TG-43 formalism: current status and recommendations for clinical implementation. *Med Phys* 2012; 39:6208–36.
31. Hyer DE, Sheybani A, Jacobson GM, et al. The dosimetric impact of heterogeneity corrections in high-dose-rate ^{192}Ir brachytherapy for cervical cancer: investigation of both conventional Point-A and volume-optimized plans. *Brachytherapy* 2012;11: 515–20.
32. Raffi JA, Davis SD, Hammer CG, et al. Determination of exit skin dose for ^{192}Ir intracavitary accelerated partial breast irradiation with thermoluminescent dosimeters. *Med Phys* 2010;37: 2693–702.
33. Richardson SL, Pino R. Dosimetric effects of an air cavity for the SAVI™ partial breast irradiation applicator. *Med Phys* 2010; 37:3919–26.
34. Kwan IS, Wilkinson D, Cutajar D, et al. The effect of rectal heterogeneity on wall dose in high dose rate brachytherapy. *Med Phys* 2009;36:224–32.
35. Kirisits C, Rivard MJ, Baltas D, et al. Review of clinical brachytherapy uncertainties: analysis guidelines of GEC-ESTRO and the AAPM. *Radiother Oncol* 2014;110:199–212.